Available online at www.sciencedirect.com

ScienceDirect

Energy Procedia 1 (2009) 3415–3419

Energy Procedia

www.elsevier.com/locate/procedia

GHGT-9

Water Reactivity in the Liquid and Supercritical CO_2 Phase: Has Half the Story Been Neglected?

B. P. McGrail[a,*], H. T. Schaef[a], V.-A. Glezakou[b], L. X. Dang[b], A. T. Owen[a]

[a]*Pacific Northwest National Laboratory, Energy & Environment Directorate, P.O. Box 999, Richland, Washington 99352, USA*
[b]*Pacific Northwest National Laboratory, Fundamental & Computational Sciences Directorate, P.O. Box 999, Richland, Washington 99352, USA*

Abstract

Aqueous-phase mediated chemical reactions with dissolved CO_2 have long been considered the principal if not only reactive process supporting mineralization reactions with basalt and other reactive reservoir rocks and caprocks in deep geologic sequestration systems. This is not surprising given the quite high solubility of CO_2 in the aqueous phase and ample evidence from natural systems of the reactivity of CO_2-charged waters with a variety of silicate minerals. In contrast, comparatively scant attention has been directed at reactivity of water solvated in liquid and supercritical CO_2, with the exception of interest in the impacts of water in CO_2 on the corrosion of pipeline steels. The results presented in this paper show that the most interesting and important aspects of water reactivity with metal and oxide surfaces of interest in geologic sequestration systems actually occurs in the liquid or supercritical CO_2 phase.

Keywords: sequestration, corrosion, carbonate precipitation, molecular dynamics

1. Introduction

The capture and storage of carbon dioxide and other greenhouse gases as supercritical fluids in deep geologic formations represents one of the most economic options allowing time for continued use of abundant fossil fuels while new technologies are developed and deployed for transportation and electric power generation [1]. Carbon capture and sequestration systems (CCS) involve a considerable number of engineered and natural components that will be exposed to and interact with CO_2 (and other components mixed with the CO_2) over long periods of time. Hence, there has been considerable work done examining interactions of CO_2 with cements used in well completion [2, 3] and a variety of minerals and rocks representative of candidate host formations [4-6] and caprocks [7]. Reactions of CO_2 with steels used in well casings and pipelines has also been studied [8-10].

Nearly all of this prior research has focused on aqueous phase mediated reactions containing dissolved CO_2 except for some limited scoping studies [11, 12]. However, as we will demonstrate in this paper, interactions with water-bearing supercritical fluids (WBSF) appear to be of equal if not more importance in CCS systems for the following reasons. First, the introduced supercritical CO_2(and other constituents) over almost all ranges of temperature and pressure relevant to geologic sequestration is less dense than the aqueous phase or brine, and this lower density will result in a migration of the supercritical fluid upwards and so dominate the contact area with the isolating caprock. Second, the injected CO_2 is likely to contain near-saturation amounts of water initially or soon after injection through absorption of connate water. The WBSF is both highly diffusive owing to its low viscosity and highly reactive owing to the potential acidic nature of water solvated in the dense CO_2–dominant phase. The high diffusion rate and correspondingly low capillary entry pressure means that these fluids can permeate into the overlying caprock pore network and access any undetected faults or fractures as well. Third, corrosion and mineral transformation reactions occurring from contact with WBSF are fundamentally different than reactions of the same materials in aqueous solutions. Specifically, well-defined concepts in aqueous solutions such as mineral solubility and ion activity do not have corresponding thermodynamic meaning in WBSFs; direct molecular interactions of the fluid phase components with the surfaces is expect to result in localized mineral replacement or transformation reactions unlike dissolution/re-precipitation reactions involving solution phase ion transport. In this paper, we will demonstrate both experimentally and computationally that WBSFs are all highly

doi:10.1016/j.egypro.2009.02.131

reactive with minerals, steels, cements, and other materials of importance in geologic sequestration systems, resulting in the key question "Has half of the story been neglected?".

2. Experimental

2.1. Steel Corrosion Experiments

Steel corrosion is an important consideration in wellbore and pipeline design where water contents in the liquid or $SCCO_2$ phase could be significantly higher than is current industry practice. For example, elimination of a chemical dehydration system could save 10's of millions of dollars in annual operating costs for a medium-sized power plant, provided the wetter CO_2 could be safely transported and injected into a storage reservoir. Experiments were conducted in specially-designed Parr reactor vessels constructed from Ti (grade IV), which is highly resistant to corrosion, and fitted with a quartz window (1.6 cm wide by 8.9 cm tall). Carbon dioxide was purchased from Oxarc Gas (Pasco, WA) with a certified moisture content of <2 ppmw. A number of tests were conducted ranging in duration from several days to two weeks. Steel coupons measuring 25 mm wide by 44 mm long and 5 mm thick were cleaned, polished with 600 grit SiC paper, and dried at 100°C for one hour prior to each experiment. Optical microphotographs were collected after the cleaning procedure to verify surface conditions. Using a small rod machined from PEEK, the steel coupons were secured against the quartz window in the reactor prior to pressurization. ISCO syringe pumps were used to deliver CO_2 into the reactor up to 7 MPa. Deionized water (DIW) was added to the vessel before the addition of CO_2. Experiments were maintained at room temperature (~25°C). Surface conditions of the steel coupon were monitored throughout the duration of the experiments by way of the quartz window. Post characterization of surface reactions included optical microscopy and x-ray diffraction (XRD).

Initial testing was conducted in a configuration where the steel coupon straddles the contact interface between the aqueous phase and liquid CO_2 phase. After placement of the steel coupon, the reactor was pressurized to 7 MPa (1000 psig) with CO_2. Liquid CO_2 filled 2/3 of the reactor, measuring 1 cm above the top steel coupon. Visible through the quartz window was the H_2O and liquid CO_2 interface positioned ~2 cm from the bottom of the coupon. After 48 hours of testing, corrosion products formed on the steel coupon in direct contact with the liquid CO_2. For example, Figure 1 shows the post-reacted surface corrosion pattern. Clearly visible is the nearly pristine surface of the portion of the steel coupon immersed in the aqueous phase. In contrast, the coupon surface immersed in liquid CO_2 (which would be saturated with water) shows extensive surface corrosion development (Figure 1).

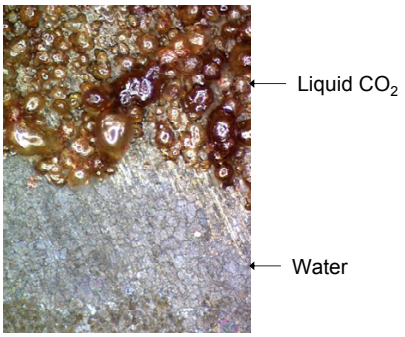

Surface characterization of the reacted coupon by XRD was conducted following the termination of the experiment. Scans were collected from 10° to 65° 2θ at 0.1° per minute. Siderite, $Fe(CO_3)$, was identified as the only crystalline reaction product. Amorphous precipitates are not detectable by XRD and should also be considered as a possible corrosion product.

Additional experiments were performed to determine the maximum concentration of dissolved H_2O in CO_2 before surface corrosion was induced on mild steel. Two experiments were performed using ANSI 01 carbon steel coupons and water concentrations at 610 ppmw and 998 ppmw, respectively. Parameters for both experiments are shown in Table 1. Coupons were washed with ethyl alcohol, triple rinsed with DIW, and oven dried at 100°C for one hour. Surfaces of the unreacted steel coupons were dominated by minor scratches, most likely the result of manufacturing processes and surface cleaning. The surfaces appeared shiny and void of any type of corrosion products.

Table 1. Parameters for high pressure CO_2-H_2O steel coupon corrosion experiments

Parameters	Vessel 1	Vessel 2
H_2O (ppmw)	610	998
H_2O (g)	0.05	0.51
CO_2 (l)[1]	64	387
Pressure (MPa)	6.25	6.32
Temperature (°C)	22	22
Duration (days)	42	21
Coupon Dimension (mm)	26.2 × 38.7 × 4.7	25.2 × 44.0 × 4.7
[1] liquid CO_2 density =751 kg/m^3		

Over the duration of the experiments, digital photographs were collected of both steel coupon surfaces through the quartz glass windows. No surface corrosion was observed during the first 48 hours of testing on either coupon. Minor surface corrosion was first observed after 72 hours testing on the steel coupon in vessel 2 (Figure 2f). Over the time span of 21 days, corrosion product steadily formed on the steel coupon in vessel 2 as can be seen in Figure 2 e-h. The experiment was terminated after 21 days. No corrosion was detected in vessel 1 even after 42 days of testing.

Under the experimental conditions (22°C, 6.3 MPa), water solubility in liquid CO_2 is approximately 1100 ppmw [13]. Consequently, corrosion is taking place in the liquid CO_2 phase when no free (unsolvated) water is present. However, a threshold water content does exist for onset of corrosion. Further experiments are needed to better define the exact value but we know that at ≤610 ppmw H_2O content in pure CO_2, no corrosion was detected even after 42 days of exposure.

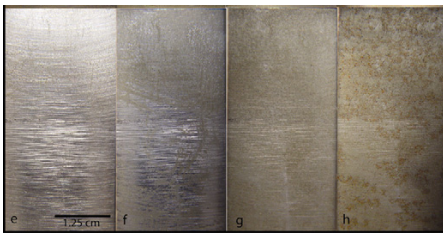

To examine corrosion behavior in the presence of molecular water solvated in liquid CO_2 containing H_2S, an experiment was conducted using premixed CO_2 with H_2S. The H_2S was introduced into a tared gas cylinder (250 ml) equipped with a low pressure gauge. After determining the weight of H_2S added, CO_2 was added to the vessel by an ISCO syringe pump until the desired weight was obtained. The CO_2-H_2S mixture was then used to pressurize a vessel containing the steel sample (X70 pipeline steel in this case) and a known amount of water. For the test reported here, the water content was 408 ppmw, H_2S content was 321 ppmw, and total pressure was 8.2 MPa. Vessels were maintained at room temperature (≈24°C) for the entire test duration of 48 days. Prior to testing, one side of the X70 steel coupon was polished as in previous tests with 600 grit SiC paper. The back side of the X70 steel coupon, however, was sand blasted, which created a rough surface.

After 48 days of testing at 24°C, the X70 coupon was removed and photographed. Figure 3 shows the smooth side (a) and sand blasted side (b). During testing, the coupon was positioned vertically in the bottom of the reactor, in direct contact with the reactor base. Corrosion appears more pronounced towards the bottom of the smooth side, with noticeably less surface alteration towards the top (Figure 3a). Horizontal bands of different colors are observable on the upper half of the coupon. In comparison, the sand blasted side of the coupon appears to have undergone extensive, uniform corrosion over the entire surface (Figure 3b). Dark precipitates with some indications of a white precipitate (towards the top of the coupon) indicating the formation of various corrosion products, perhaps different than what was observed on the smooth surface (Figure 3a).

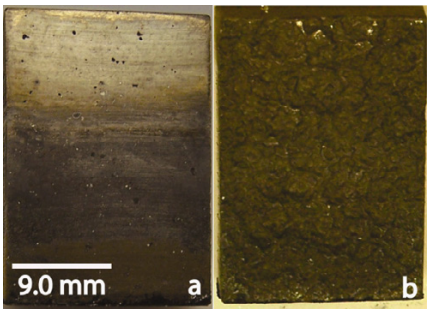

Figure 3. Precipitate on X70 steel coupon after 49 days of testing (8.2 MPa CO_2, 321 ppm H_2S, 408 ppm H_2O, 24°C)

2.2. Whole Rock Experiments

To determine whether water solvated in the CO_2 phase is as reactive with silicate minerals as was observed with steel, a series of similar experiments was performed with basalt samples. Prior work has demonstrated the relatively rapid mineralization that occurs with basalt samples submerged in water that is in equilibrium with $SCCO_2$ [4, 14]. In these experiments, we investigate whether mineralization can also take place directly with the SCCO2 phase.

Pieces of Columbia River Basalt (CRB) and Newark Basin (NB) basalt were exposed to water-saturated $SCCO_2$ at 10.34 MPa and 50°C. The samples were configured in a pressure vessel such that the bottom of the sample was immersed in the water phase with the remaining portion of the sample exposed only to the SCCO2 phase. No attempts were made to mechanically mix the two fluids – transfer of water into the CO_2 phase was allowed to occur by diffusion and natural convective mixing only. Two of the four reactors were terminated after 95 days of testing and the reacted basalt samples were examined for carbonate precipitates.

The dark flat surface of the NB sample was characterized using an optical microscope. White carbonate precipitate was visible on the NB basalt (Figure 4a), both on the lower 1 cm section of sample that was submerged in water, and on the upper section that was above the water line and only exposed to $SCCO_2$. In the SEM, the carbonate appears dark (Figure 4b) and the basalt grains appear bright, revealing an Fe-rich phase of the basalt. Chemistry of the precipitates, obtained by SEM energy dispersive x-ray spectroscopy (EDXS) indicated calcium rich areas or typical basalt chemistry enriched in Fe and Ca. The EDXS analysis did reveal Cl in the precipitates above the water line, but was absent in the carbonate precipitates below the water line. In the aqueous phase, the Cl enters the solution in contact with basalt as a highly soluble anion. However in the SCCO2 phase, water is present only as solvated molecular species, i.e. there is no aqueous phase to accommodate the Cl and so it is incorporated in the carbonate phase.

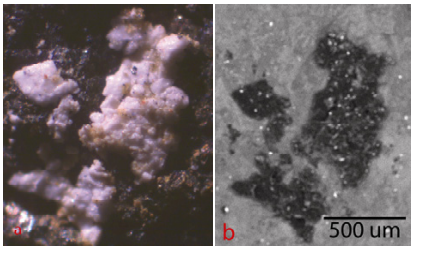

Figure 4. Carbonate precipitate with small basalt grains on the surface of NB basalt above the water line as seen with a) optical microscopy and b) scanning electron microscopy (10.34 MPa CO_2, 50°C, 95 days).

Other experiments were performed with the NB basalt suspended above the water phase in the pressure vessel to eliminate the chance of surface diffusion of free water influencing the mineralization behavior. Carbonate minerals were again observed in this configuration. Metal oxides ($TiFeO_2$) were incorporated into these

precipitates suggesting carbonate directly replaced the glassy mesostasis. Clearly, molecular water in the SCCO2 phase is ubiquitously reactive, i.e. corrosion of mild steel in WBSFs is not a unique phenomenon.

3. Discussion

The implications of the chemical reactivity of water dissolved in the dense CO_2 phase are potentially far reaching. Supercritical CO_2 migrating through undetected cracks and fractures in caprocks could, in theory, self seal over time through mineralization reactions taking place with the water carried by the CO_2 itself. Also, we are not aware of any reservoir simulator at this time with capabilities to model water absorption and subsequent reactivity on mineral surfaces occurring directly with liquid or supercritical CO_2. Mineral transformation reactions occurring in WBSFs are fundamentally different than reactions of the same mineral in aqueous solutions. Specifically, well-defined concepts in aqueous solutions such as mineral solubility and ion activity do not have corresponding thermodynamic meaning in liquid or SCCO2-dominated fluids; direct molecular interactions of the fluid phase components with mineral surfaces results in localized mineral replacement or transformation reactions unlike dissolution/re-precipitation reactions involving solution phase ion transport. Significant code development and parameterization would appear to be required to enable modeling molecular water interactions with silicate minerals leading to carbonate mineral formation.

Molecular dynamics (MD) simulations can be used to aid in the understanding of the role of CO_2 and molecular water solvated in CO_2 on corrosion and mineralization processes. For example, Nassir and Dwyer [15] showed evidence of CO_2 adsorption and subsequent cleavage of CO_2 upon adsorption on iron surfaces. As a first step, we employed DFT-based quantum mechanical calculations to study the reaction of CO_2 with the 100 surface on α-Fe. In agreement with the literature, we find that CO_2 forms several stable (negative binding energies) bound species, as shown in Figure 5 and Table 2. Subsequent C-O cleavage of the adsorbed species has a barrier of about 7 kcal/mol correlating with the strongly bound O and CO. Reaction of adsorbed O with another CO_2 is likely to proceed without a barrier and results in the formation of CO_3 (Figure 6).

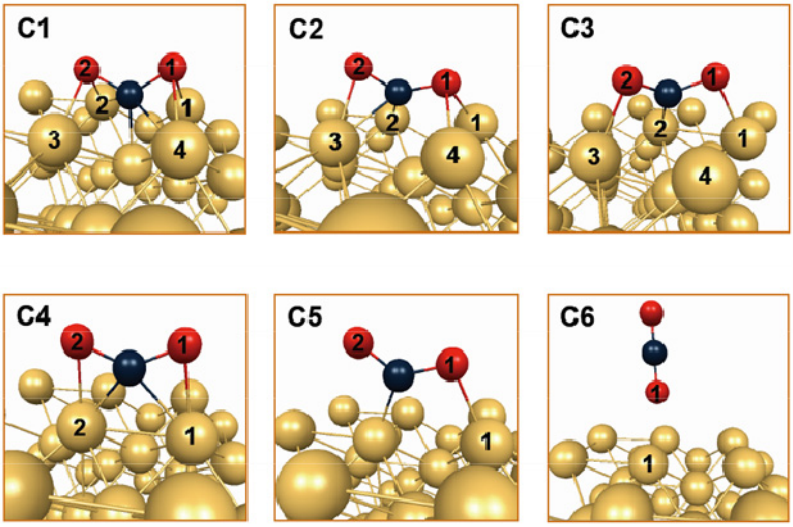

Figure 5. CO_2 configurations on Fe(100)

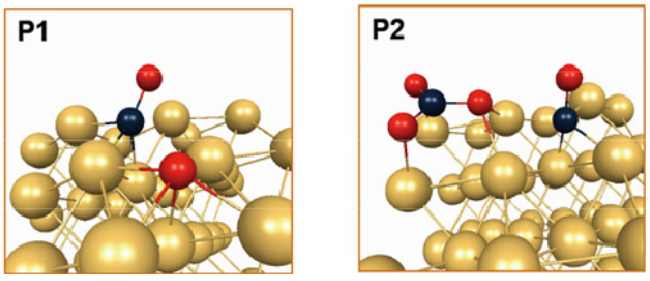

Figure 6. -O cleavage of adsorbed CO_2 (P1), and CO_3 formation (P2)

In all cases of chemisorbed CO_2 (Figure 5, panels C1-C5), we see that it is stabilized on the surface with multiple bonds that, in most cases, involve all 3 centers of CO_2. Calculated binding energy for each of these configurations is given in Table 2 . The most stable configuration, C1, binds by 16.7 kcal/mol. We notice that this configuration has the longest C-O bonds, indicating that longer, weaker C-O bonds facilitate multiple interaction with the surface. The stronger C-Fe and O-Fe bonds lead to a more strongly bound system. Physisorbed CO_2 (C6) has a repulsive interaction with the surface, reflected in a slight shortening of the CO bond closest to the surface, and overall becomes destabilized compared to the non-interacting surface+CO_2.

Table 2. Binding energies of CO_2, CO+O and CO_3. Energies are calculated as differences of E(slab+adsorbate)-E(slab)-E(adsorbate), in eV

Species	BE(eV)
C1	-0.73
C2	-0.63
C3	-0.71
C4	-0.52
C5	-0.56
C6	+0.4
P1	-1.21
P2	-2.51

In this study, we also computed the dissociation process of adsorbed CO_2 on Fe(100) and found that the dissociated species OC+O/Fe(100) is more stable by 11.3 kcal/mol compared to the most stable C1 configuration. Both O and CO are approximately situated at 4-fold sites. The C-O distance changes from ~1.35 Å in the chemisorbed CO_2 to almost 3.0 Å in the dissociated state (see Figure 6, panel P1). Hence, based on this periodic slab model, CO_2 gets spontaneously activated when in proximity with a clean Fe(100) surface and is thermodynamically favorable to dissociate and react with other adsorbed CO_2 molecules to produce corrosion products, $FeCO_3$, in neat CO_2. However, our experiments show that water plays an essential role in enabling the corrosion process to continue past the first monolayer type interactions being evaluated in these initial simulations. Additional work that accounts for water transport mechanisms deeper into the iron surface is needed.

4. Conclusion

Both experiments and molecular dynamics simulations show that molecular water solvated in liquid and supercritical CO_2 is quite reactive towards both iron and silicate mineral surfaces under conditions that approximate those anticipated for carbon capture and geologic sequestration systems. The presence of contaminants in the CO_2, such as H_2S, appears to significantly affect reactivity as well. Additional attention is warranted in studying potential impacts of water in the supercritical phase on the major surface and subsurface components deployed for CCS. Collectively, surface-fluid interactions with the water-bearing SCCO2-dominated fluids are pivotal and could result in the stable sequestration of CO_2 by trapping in mineral phases such as carbonates, and plugging of undetected faults or fractures in the overlying rock strata. On the other hand, corrosion of well casing materials and mechanical degradation of cements used in well completion also need to be examined in light of this evidence for the remarkable reactivity of water solvated in supercritical CO_2.

Acknowledgements

The authors wish to acknowledge Nat Saenz for his assistance in conducting the SEM analysis discussed in this paper. This work was funded by the U.S. Department of Energy, Office of Fossil Energy through the Zero Emission Research & Technology Center directed by Montana State University. The Pacific Northwest National Laboratory is operated by Battelle Memorial Institute for the United States Department of Energy under Contract DE-AC05-76RL0 1830.

5. References

1. J. A. Edmonds, P. Freund and J. J. Dooley, "The Role of Carbon Management Technologies in Addressing Atmospheric Stabilization of Greenhouse Gases," in Proceedings of the Fifth International Conference on Greenhouse Gas Control Technologies D. J. Williams, R. A. Durie, P. McMullan, C. A. J. Paulson and A. Y. Smith, Eds., pp. 46-51, CSIRO Publishing, Collingwood, Australia (2001).
2. J. W. Carey, M. Wigand, S. J. Chipera, G. WoldeGabriel, R. Pawar, P. C. Lichtner, S. C. Wehner, M. A. Raines and G. D. Guthrie, International Journal of Greenhouse Gas Control 1 (2007) 75-85.
3. M. A. Venhuis and E. J. Reardon, Environ. Technol. 24 (2003) 877-887.
4. B. P. McGrail, H. T. Schaef, A. M. Ho, Y. J. Chien, J. J. Dooley and C. L. Davidson, J. Geophys. Res.-Solid Earth 111 (2006)
5. T. F. Xu, J. A. Apps and K. Pruess, J. Geophys. Res.-Solid Earth 108 (2003)
6. Y. K. Kharaka, D. R. Cole, S. D. Hovorka, W. D. Gunter, K. G. Knauss and B. M. Freifeld, Geology 34 (2006) 577-580.
7. I. Gaus, M. Azaroual and I. Czernichowski-Lauriol, Chem. Geol. 217 (2005) 319-337.
8. M. Nordsveen, S. Nešić, R. Nyborg and A. Stangeland, Corrosion 59 (2003) 443-456.
9. Z. D. Cui, S. L. Wu, S. L. Zhu and X. J. Yang, Appl. Surf. Sci. 252 (2006) 2368-2374.
10. A. Ikeda, J. Jpn. Pet. Inst. 45 (2002) 55-69.
11. H. Lin, T. Fujii, R. Takisawa, T. Takahashi and T. Hashida, J. Mater. Sci. 43 (2008) 2307-2315.
12. O. Regnault, V. Lagneau, H. Catalette and H. Schneider, Comptes Rendus Geoscience 337 (2005) 1331-1339.
13. N. Spycher, K. Pruess and J. Ennis-King, Geochim. Cosmochim. Acta 67 (2003) 3015-3031.
14. A. P. Gysi and A. Stefansson, Mineral. Mag. 72 (2008) 55-59.
15. M. H. Nassir and D. J. Dwyer, J. Vac. Sci. Tech. A 11 (1993) 2104-2109.